molbank

MDPI

Communication

Crystal Structure of a Chiral *Sec*-Amine, 4-Chloro-*N*-(1-(pyridin-2-yl)ethyl)aniline

Adesola A. Adeleke [1,2] and Bernard Omondi [1,*]

[1] School of Chemistry and Physics, University of Kwazulu-Natal, Pietermaritzburg Campus, Private Bag X01, Scottsville 3209, South Africa; 217080311@stu.ukzn.ac.za
[2] Department of Chemical Sciences, Olabisi Onabanjo University, Ago-Iwoye, P. M. B. 2002, Ogun State 120107, Nigeria
* Correspondence: owaga@ukzn.ac.za

Abstract: In this communication, we present the crystal structure of a secondary amine: 4-chloro-*N*-(1-(pyridin-2-yl)ethyl)aniline (L_b) obtained from a stepwise reduction of an imine, (*E*)-*N*-(4-chlorophenyl)-1-(pyridin-2-yl)ethan-1-imine (L_a) with sodium borohydride. The structure was characterized by FT-IR, ^{1}H and ^{13}C NMR, Mass Spectroscopy and X-ray diffraction.

Keywords: $NaBH_4$; chiral; *sec*-amine; reductive amination; crystal structure; imines

Citation: Adeleke, A.A.; Omondi, B. Crystal Structure of a Chiral *Sec*-Amine, 4-Chloro-*N*-(1-(pyridin-2-yl)ethyl)aniline. *Molbank* **2022**, *2022*, M1335. https://doi.org/10.3390/M1335

Academic Editor: R. Alan Aitken

Received: 1 January 2022
Accepted: 7 February 2022
Published: 9 February 2022

1. Introduction

Schiff bases are a significant ligand in synthetic chemistry due to their numerous applications [1–3]. The capacity of the Schiff bases C=N double bond to be reduced to a C-N single bond to generate their corresponding secondary amine is one of their most intriguing properties. *Sec*-amines are crucial synthesis intermediates in the pharmaceutical [4], polymer [5] and agricultural [6] sectors. Most *sec*-amines can be made either by direct reductive amination of carbonyl compounds or via a stepwise reaction that starts with the synthesis of imines and then reduces them to amines. The stepwise procedure in reducing imines to amines is a commonly used approach to avoid overalkylation and direct reduction of carbonyl compounds to the appropriate alcohol. It requires the use of various metal hydrides reagents such as Bu_2SnClH [7], $LiAlH_4$ [8], $(g\text{-}C_5H_5)_2MoH_2$ [9], CaH_2/ZnX_2 [10] and $NaBH_4$ [11]. Most of these metal hydrides have chemoselective limitations, low yields and are expensive. As a result, most studies utilize sodium borohydrides [12] or its modified compounds such as $Na(CH_3COO)_3BH$ [13], $NaBH_3CN$ [14], $NaBH(OAc)_3$ [15] and $Zn(BH_4)_2$ [16] to reduce imines to *sec*-amines. The choice of sodium borohydride is related to it being a highly selective reducing agent that won't attack other functional groups in a molecule. As such, sodium borohydride ($NaBH_4$) was employed in this study to reduce (*E*)-*N*-(4-chlorophenyl)-1-(pyridin-2-yl)ethan-1-imine Schiff base to the title *sec*-amine.

2. Results

The reduction of imine (*E*)-*N*-(4-chlorophenyl)-1-(pyridin-2-yl)ethan-1-imine (L_a) with $NaBH_4$ in methanol solvent led to the formation of a yellow crystal *sec*-amine of 4-chloro-*N*-(1-(pyridin-2-yl)ethyl)aniline (L_b). The known compound [17] was obtained in a simple stepwise reductive process with a high yield. The formation of the compound was revealed by the appearance of a new quartet in the ^{1}H NMR spectrum of L_b (Figure S1), which was attributed to the proton attaching to the methyl group at δ 4.57 ppm. The ^{13}C NMR spectrum (Figure S2) further confirmed the formation of L_b. In the FT-IR spectrum of the title amine (Figure S3), the appearance of strong absorption bands at 3264 cm^{-1} assigned to the -NH group clearly shows the successful reduction of the imine C=N double bond to amine C-N single bond. The peak at 1339, 1286 and 1235 cm^{-1} corresponding to the

vibrational signals of the C-N single bond also confirm the presence of the new C-N single bond. The peak at 741 cm^{-1} can be assigned to the C-Cl vibration signal.

The molecular structure of L_b was further confirmed by X-ray crystallography. L_b was crystallized from methanol to obtain yellow needle-like crystals suitable for X-ray crystallography. The crystal structure of L_b (Figure 1) revealed that it belongs to the monoclinic system with the space group *P*21/*c*. The plane of the pyridinyl moiety is connected to that of the phenyl ring by an NH-CH-CH_3 linker with a torsional angle of 63.0 (2)° between them. The bond length of the amino N1-C4 (1.38 (2) Å) and the phenyl ring C, as well as the bond length of the amino N1-C5 (1.45 (2) Å) (Table 1) and the chiral center, are both close to the average C-N single bond length [18,19]. The chiral *sec*-amine L_b has a distorted tetrahedral structure, and its geometrical parameters (Table 1) are similar to the literature report [20]. The packing structure of L_b (Figure 2a) also showed strong H-N· · · · · N_{py} intermolecular interactions forming its dimer structure (Figure 2b). Notable weak C-H· · · · · Cl and N_{py}· · · · · H-N intermolecular hydrogen bonds were also seen.

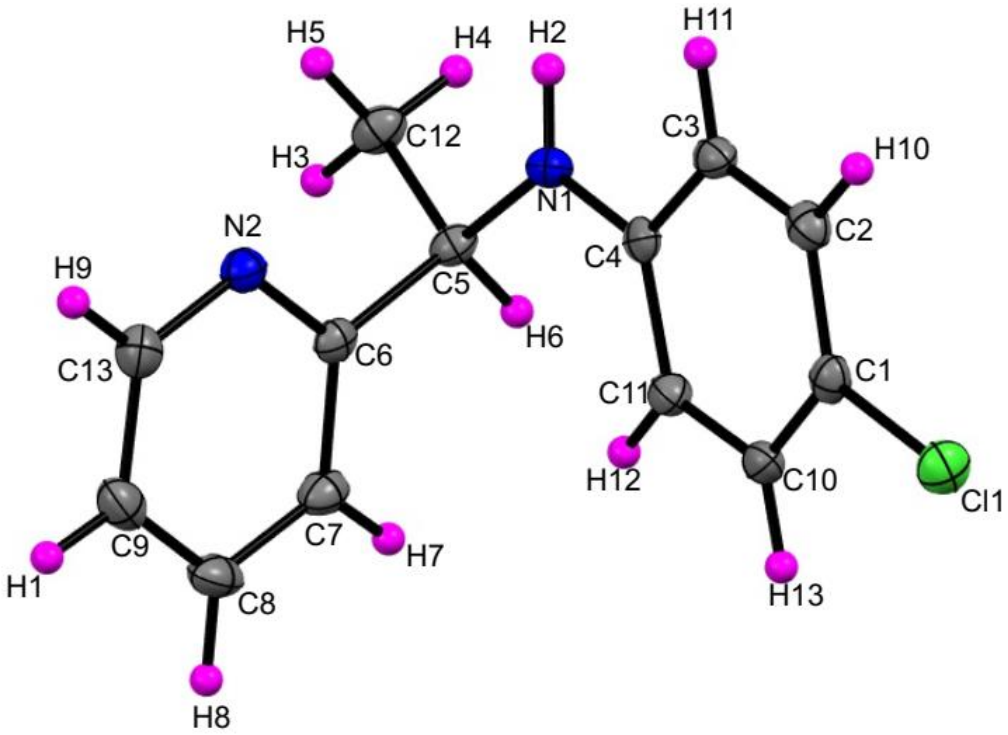

Figure 1. The ORTEP diagrams of L_b with the thermal ellipsoids drawn at the 50%. Atoms color: (a) blue = nitrogen, (b) pink = hydrogen, (c) green = chlorine, (d) grey = carbon.

Table 1. Selected geometric parameters for L_b.

Atom	Length/Å	Atom	Angle/°
N(1)-C(5)	1.45 (2)	C(12)-C(5)-N(1)	108.34 (12)
H(6)-C(5)	1.00	H(6)-C(5)-C(6)	108.43
C(12)-C(5)	1.53 (2)	H(6)-C(5)-N(1)	108.43
C(6)-C(5)	1.53 (2)	H(6)-C(5)-C(12)	108.43
C(1)-Cl(1)	1.76 (2)	C(6)-C(5)-C(12)	110.18 (12)
		N(1)-C(5)-C(6)	112.93 (12)

D-H . . . A	d(D-H)/Å	d(H . . . A)/Å	d(D . . . A)/Å	<D-H-A/°
N(1)-H(1) . . . N(21)	0.88	2.25	3.08 (17)	158.3
C(2)-H(2) . . . Cl(12)	0.95	2.97	3.88 (15)	160.5
C(10)-H(10) . . . Cl(13)	0.95	2.91	3.75 (15)	148.3
C(13)-H(13) . . . Cl(14)	0.95	2.99	3.91 (16)	163.8

[1]2-x, -y, 1-z; [2]1-x, -y, 2-z; [3]+x, $\frac{1}{2}$-y, -$\frac{1}{2}$ + z; [4]1 + x, +y, +z

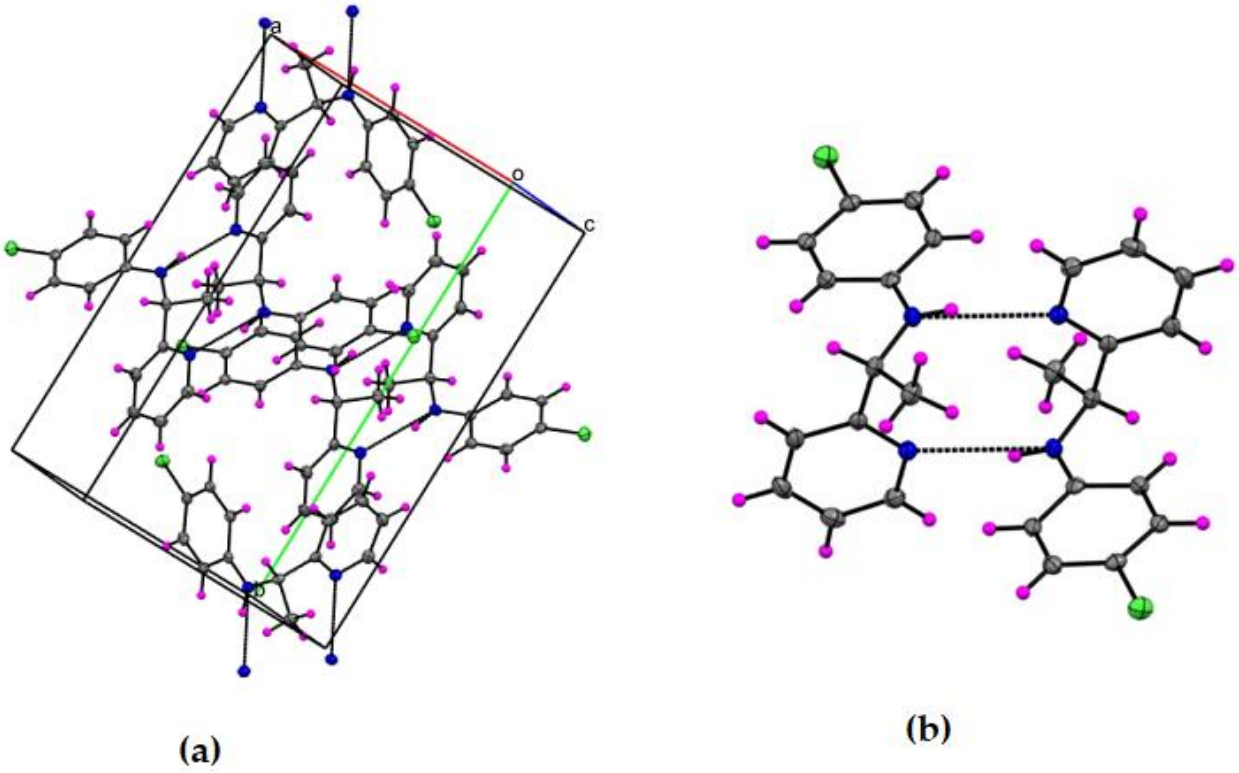

Figure 2. (**a**) The view of packing the diagram of L_b molecules along the b axis. (**b**) A nitrogen-bonded dimer structure of L_b formed via intermolecular H-N· · · · · N nitrogen bonds. Atoms color: (a) blue = nitrogen, (b) pink = hydrogen, (c) green = chlorine, (d) grey = carbon.

3. Materials and Methods

Methanol 99.5% (Aldrich, St. Louis, MO, USA), ethyl acetate 99.8% (Aldrich, St. Louis, MO, USA), 2-pyridinecarboxaldehyde 99% (Aldrich, St. Louis, MO, USA), 4-chloroaniline 99% (Aldrich, St. Louis, MO, USA) and $NaBH_4 \geq 98\%$ (Aldrich, St. Louis, MO, USA) were purchased from local suppliers. All chemicals were of analytical grade and were used as they were given to us. On a BRUKER 400 MHz spectrometer (Karlsruh, German), ^1H NMR and ^{13}C NMR spectra in $CDCl_3$ were recorded. Chemical shift values in $CDCl_3$ are expressed in parts per million (ppm) in relation to the solvent residual peaks; 7.26 ppm for ^1H NMR and 77.16 ppm for ^{13}C NMR. In ^1H NMR spectrum, the splitting pattern is designated as s for singlet, d for doublet, m for multiplet and *J* for joint (the coupling constant is given in Hertz). The infrared spectrum was recorded using a PerkinElmer Spectrum 100 FT-IR spectrometer (Waltham, MA, USA), and the data were reported as percentage transmittances at the respective wavenumbers (cm^{-1}), between 4000 and 650 cm^{-1}. Only molecular ions (M+) and major fragmentation peaks were reported in the mass spectrum, with intensities expressed as percentages of the base peak, using the Shimadzu LCMS-2020 instrument (Kyoto, Japan).

3.1. Synthesis of 4-chloro-*N*-(1-(pyridin-2-yl)ethyl)aniline L_a

A known ligand (*E*)-*N*-(4-chlorophenyl)-1-(pyridin-2-yl)ethan-1-imine (L_a) [21] was first synthesized using methods similar to our earlier reports [22,23]. Afterward, L_a was reduced to a secondary ligand 4-chloro-*N*-(1-(pyridin-2-yl)ethyl)aniline (L_b) (Scheme 1) using a modified method from the literature [24].

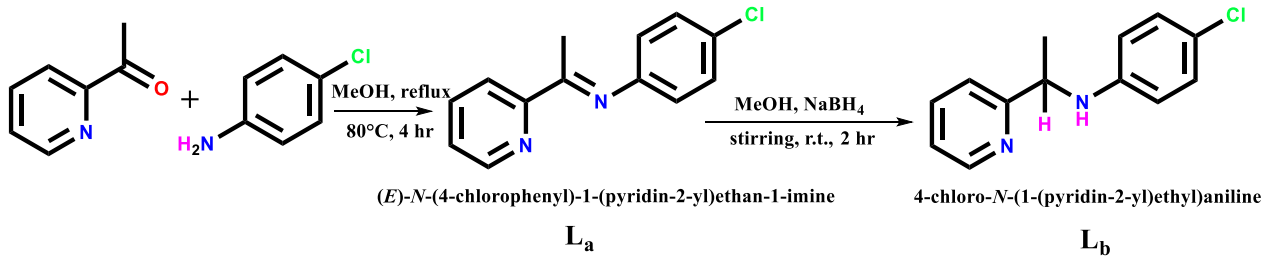

Scheme 1. Synthesis of the secondary amine (L_b) from imine (L_a).

Synthesis of the secondary amine L_b: The yellow (*E*)-*N*-(4-chlorophenyl)-1-(pyridin-2-yl)ethan-1-imine, L_a (1.15 g, 5 mmol) was dissolved in methanol (100 mL) with vigorous stirring and $NaBH_4$ (0.19 g, 5 mmol) was added gradually within 15 min until the solution became colorless. The resulting solution was further stirred for another 2 h at room temperature. Afterward, the methanol was removed in vacuo. The residue was dissolved in Ethyl acetate washed with cold water (3 × 100 mL). The Ethyl acetate was dried with $MgSO_4$, filtered and the solvent removed in vacuo to afford an oil product. The resultant yellow oil was heated in a small amount of methanol and allowed to slowly evaporate at room temperature, yielding a crystalline product that was recrystallized from methanol. M.p. 105 °C [17], Yield: 0.91 g, 78%, ^{1}H-NMR (400 MHz, $CDCl_3$, δ ppm): 8.56 (d, *J* = 4.0 Hz, 1H, Hd-py), 7.61 (dd, *J* = 8.0 Hz, *J* = 7.9 Hz, 1H, Hb-py), 7.30 (d, *J* = 7.9 Hz, 1H, Ha-py), 7.15 (dd, *J* = 8.0 Hz, *J* = 4.0 Hz, 1H, Hc-py), 7.09 (d, *J* = 8.8 Hz, 1H, Hi or Hj), 7.05 (d, *J* = 8.8 Hz, 1H, Hi or Hj), 6.60 (d, *J* = 8.9 Hz, 1H, Hh or Hk), 6.48 (d, *J* = 8.9 Hz, 1H, Hh or Hk), 4.57 (q, *J* = 6.7 Hz, 1H, He-CH), 1.53 (d, *J* = 6.7 Hz, 3H, Hf-CH_3). ^{13}C-NMR (100 MHz, $CDCl_3$, 25 °C): δ = 149.34 (C5-py), 145.77 (C8-C_6H_4), 145.10 (C1-py), 129.23 (C11-C_6H_4), 129.11 (C12-C_6H_4), 123.29 (C3-py), 122.29 (C4-py), 122.14 (C13-C_6H_4), 120.54 (C2-py), 116.35 (C10-C_6H_4), 114.67 (C9- C_6H_4), 54.87 (C7-CH), 23.17 (C6-CH_3). FT-IR (cm^{-1}): 3264, 3052, 1598, 1339, 1286, 1235, 743.

3.2. X-ray Crystallography

A Bruker Apex Duo diffractometer with an Oxford Instruments Cryojet running at 100 (2) K and an Incoatec micro source working at 30 W power was used to evaluate and collect data of L_b. The data were collected with Mo Kα (λ = 0.71073 Å) radiation at a crystal-to-detector distance of 50 mm using omega and phi scans. The data were reduced with the program SAINT [25] using outlier rejection, scan speed scaling, as well as standard Lorentz and polarization correction factors. A SADABS [26] semi-empirical multi-scan absorption correction was applied to the data. The structure of the ligand L_b was solved by the direct method using the SHELXS [27] program and refined. The visual crystal structure information was performed using ORTEP-3 [28], program. Non-hydrogen atoms were first refined isotropically and then by anisotropic refinement with a full-matrix least-squares method based on F^2 using SHELXL [29]. All hydrogen atoms were positioned geometrically, allowed to ride on their parent atoms and refined isotropically. The crystallographic data and structure refinement parameters of the *sec*-amine L_b are given in Table 2.

Table 2. Crystal data and structure refinement for L_b.

	L_b
Chemical formula	$C_{13}H_{13}ClN_2$
Formula Weight	232.70
Crystal system	Monoclinic
Space group	*P* 21/c
a (Å)	9.4547 (5)
b (Å)	16.2237 (8)

Table 2. *Cont.*

	$\mathbf{L_b}$
c (Å)	7.9004 (4)
α (°)	90
β (°)	104.169 (3)
γ (°)	90
V (Å^3)	1174.98 (10)
Z	4
ρ_{calc} (g cm^{-3})	1.315
μ (mm^{-1})	0.298
F (000)	488.0
Crystal size (mm^3)	0.660 × 0.280 × 0.220
θ range for data collection (°)	2.222 to 26.718
Index ranges	$-11 \leq h \leq 11$, $-19 \leq k \leq 20$, $-9 \leq l \leq 9$
Reflections collected	16177
Independent reflections	2480 [R (int) = 0.0341]
Completeness to theta = 25.242	99.9%
Data/restraints/parameters	2480/0/146
Goodness-of-fit on F^2	1.101
R indices [I > 2sigma (I)]	R_1 = 0.0332, wR_2 = 0.0800
R indices (all data)	R_1 = 0.0375, wR_2 = 0.0829
Largest diff. peak and hole (e Å^{-3})	0.433 and –0.467

4. Conclusions

In a two-step approach, we were able to produce a *sec*-amine with halogen functionality. Because of its high chemo-selectivity, the use of an equimolar amount of sodium borohydride in methanol aids in the effective synthesis of the chlorine-containing *sec*-amine. The *sec*-amine possesses a chiral center and forms a distorted tetrahedral structure with the chiral center.

Supplementary Materials: The following are available online. Figure S1: 1H NMR spectrum of Lb, Figure S2: 13C NMR spectrum of Lb, Figure S3: IR spectrum of Lb and Mass Spec. spectrum of Lb.

Author Contributions: B.O. conceived and designed the structure; A.A.A. completed the synthesis, crystal growth, characterization and manuscript drafting; B.O. revised the manuscript. All authors have read and agreed to the published version of the manuscript.

Funding: This research was funded by the National Research Foundation of South Africa (Grant number: 119342).

Data Availability Statement: CCDC No. 2131918 contains the supplementary crystallographic data for the title compound. These data can be obtained free of charge via http://www.ccdc.cam.ac.uk/conts/retrieving.html (accessed on 31 November 2021) or from the Cambridge Crystallographic Data Centre, 12 Union Road, Cambridge CB2 1EZ, UK; fax: (+44)1223-336-033 or via email: deposit@ccdc.cam.ac.uk.

Acknowledgments: The authors are grateful to the National Research Foundation and the University of KwaZulu-Natal for their financial support and for providing the Lab where this research was conducted.

Conflicts of Interest: The authors declare no conflict of interest.

References

1. Uddin, M.N.; Ahmed, S.S.; Alam, S.M.R. Biomedical applications of Schiff base metal complexes. *J. Coord. Chem.* **2020**, *73*, 3109–3149. [CrossRef]
2. Kajal, A.; Bala, S.; Kamboj, S.; Sharma, N.; Saini, V. Schiff Bases: A Versatile Pharmacophore. *J. Catal.* **2013**, *2013*, 1–14. [CrossRef]
3. Ebosie, N.P.; Ogwuegbu, M.O.C.; Onyedika, G.O.; Onwumere, F.C. Biological and analytical applications of Schiff base metal complexes derived from salicylidene-4-aminoantipyrine and its derivatives: A review. *J. Iran. Chem. Soc.* **2021**, *18*, 3145–3175. [CrossRef]
4. Patil, M.D.; Grogan, G.; Bommarius, A.S.; Yun, H. Oxidoreductase-Catalyzed Synthesis of Chiral Amines. *ACS Catal.* **2018**, *8*, 10985–11015. [CrossRef]
5. Froidevaux, V.; Negrell, C.; Caillol, S.; Pascault, J.-P.; Boutevin, B. Biobased Amines: From Synthesis to Polymers; Present and Future. *Chem. Rev.* **2016**, *116*, 14181–14224.
6. Xu, S.; Zeng, X.; Dai, S.; Wang, J.; Chen, Y.; Song, J.; Shi, Y.; Cheng, X.; Liao, S.; Zhao, Z. Turpentine Derived Secondary Amines for Sustainable Crop Protection: Synthesis, Activity Evaluation and QSAR Study. *J. Agric. Food Chem.* **2020**, *68*, 11829–11838. [CrossRef] [PubMed]
7. Kato, H.; Shibata, I.; Yasaka, Y.; Tsunoi, S.; Yasuda, M.; Baba, A. The Reductive Amination of Aldehydes and Ketones by Catalytic Use of Dibutylchlorotin Hydride Complex. *Chem. Commun.* **2006**, *40*, 4189–4191. [CrossRef]
8. Elsen, H.; Färber, C.; Ballmann, G.; Harder, S. $LiAlH_4$: From Stoichiometric Reduction to Imine Hydrogenation Catalysis. *Angew. Chem.* **2018**, *130*, 7274–7278. [CrossRef]
9. Ito, T.; Yamaguchi, Y. Syntheses and Reactivity of Group 6 Metallocene-Type Complexes Based on Bis(η-cyclopentadienyl) molybdenum and -tungsten Fragments. *J. Synth. Org. Chem. Jpn.* **2004**, *62*, 214–225. [CrossRef]
10. Aida, T.; Kuboki, N.; Kato, K.; Uchikawa, W.; Matsuno, C.; Okamoto, S. Use of CaH_2 as a reductive hydride source: Reduction of ketones and imines with CaH_2/ZnX_2 in the presence of a Lewis acid. *Tetrahedron Lett.* **2005**, *46*, 1667–1669. [CrossRef]
11. Billman, J.H.; Diesing, A.C. Reduction of Schiff Bases with Sodium Borohydride. *J. Org. Chem.* **1957**, *22*, 1068–1070. [CrossRef]
12. Tabane, T.H.; Singh, G.S. A Simple Reduction of Imines to Biologically Important Secondary Amines Using Sodium Borohydride/Alumina in Solid-Phase. *Proc. Natl. Acad. Sci. India Sect. A Phys. Sci.* **2014**, *84*, 517–521. [CrossRef]
13. Abdel-Magid, A.F.; Carson, K.G.; Harris, B.D.; Maryanoff, C.A.; Shah, R.D. Reductive Amination of Aldehydes and Ketones with Sodium Triacetoxyborohydride. Studies on Direct and Indirect Reductive Amination Procedures1. *J. Org. Chem.* **1996**, *61*, 3849–3862. [CrossRef] [PubMed]
14. Juru, A.U.; Cai, Z.; Jan, A.; Hargrove, A.E. Template-guided selection of RNA ligands using imine-based dynamic combinatorial chemistry. *Chem. Commun.* **2020**, *56*, 3555–3558. [CrossRef] [PubMed]
15. Gutierrez, C.D.; Bavetsias, V.; McDonald, E. $TiCl(O^iPr)_3$ and $NaBH(OAc)_3$: An efficient reagent combination for the reductive amination of aldehydes by electron-deficient amines. *Tetrahedron Lett.* **2005**, *46*, 3595–3597. [CrossRef]
16. Gama, I.L. Zinc Borohydride. *Synlett* **2012**, *23*, 642–643. [CrossRef]
17. Berger, L.; Corraz, A.J. 5-(Pyridylalkyl)-Pyridoindole Derivatives. U.S. Patent No. 3,522,262, 28 July 1970.
18. Dey, S.; Panda, S.; Ghosh, P.; Lahiri, G.K. Electronically Triggered Switchable Binding Modes of the C-Organonitroso (ArNO) Moiety on the $\{Ru(acac)_2\}$ Platform. *Inorg. Chem.* **2019**, *58*, 1627–1637. [CrossRef]
19. Xu, J.; Wang, L.; Liang, G.; Bai, Z.; Wang, L.; Xu, W.; Shen, X. Density Functional Theory Study on Triphenylamine-based Dye Sensitizers Containing Different Donor Moieties. *Bull. Korean Chem. Soc.* **2010**, *31*, 2531–2536. [CrossRef]
20. Biçer, A.; Kaya, R.; Yakalı, G.; Gültekin, M.S.; Cin, G.T.; Gülçin, I. Synthesis of novel β-amino carbonyl derivatives and their inhibition effects on some metabolic enzymes. *J. Mol. Struct.* **2020**, *1204*, 127453. [CrossRef]
21. Fedushkin, I.L.; Nikipelov, A.S.; Morozov, A.G.; Skatova, A.A.; Cherkasov, A.V.; Abakumov, G.A. Addition of Alkynes to a Gallium Bis-Amido Complex: Imitation of Transition-Metal-Based Catalytic Systems. *Chem. Eur. J.* **2012**, *18*, 255–266. [CrossRef]
22. Adeleke, A.A.; Zamisa, S.J.; Omondi, B. Crystal structure of 4-(1-phenylimidazo[1,5-a]pyridin-3-yl)benzoic acid ($C_{20}H_{14}N_2O_2$). *Z. Für Krist. New Cryst. Struct.* **2019**, *234*, 1157–1159.
23. Adeleke, A.A.; Zamisa, S.J.; Omondi, B. Crystal structure of dichlorido-bis((E)-2-((pyridin-4-ylmethylene)amino)phenol)zinc(II), $C_{24}H_{20}Cl_2N_4O_2Zn$. *Z. Für Krist. New Cryst. Struct.* **2020**, *235*, 625–628. [CrossRef]
24. Hamadi, H.; Javadi, S. One-pot Reductive Amination of Carbonyl Compounds with $NaBH_4$-$B(OSO_3H)_3/SiO_2$ in Acetonitrile and in Solvent-free Condition. *J. Chem. Sci.* **2017**, *129*, 75–80. [CrossRef]
25. SAINT, B. *(V7.68A), Data Reduction Software*; Bruker AXS Inc.: Madison, WI, USA, 2009.
26. Bruker, A. *(V7.60A), Saint and SADABS*; Bruker AXS Inc.: Madison, WI, USA, 2009.
27. Sheldrick, G.M. Crystal structure solution with ShelXT. *Acta Crystallogr. A* **2015**, *71*, 3–8. [CrossRef] [PubMed]
28. Farrugia, L.J. WinGX and ORTEP for Windows: An update. *J. Appl. Cryst.* **2012**, *45*, 849–854. [CrossRef]
29. Sheldrick, G.M. Crystal structure refinement with SHELXL. *Acta Crystallogr. Sect. C Struct. Chem.* **2015**, *71*, 3–8. [CrossRef] [PubMed]